

Roles of Three Well-Conserved Arginine Residues in Mediating the Catalytic Activity of Tobacco Acetohydroxy Acid Synthase

Dung Tien Le^{1,*}, Moon-Young Yoon², Young Tae Kim³ and Jung-Do Choi^{1,†}

¹School of Life Sciences, Chungbuk National University, Cheongju 361-763, Korea; ²Department of Chemistry, Hanyang University, Seoul 133-791, Korea; and ³Department of Microbiology, Pukyong National University, Busan 608-737, Korea

Received March 3, 2005; accepted April 3, 2005

Acetohydroxy acid synthase (AHAS, EC 2.2.1.6; also known as acetolactate synthase, ALS) catalyzes the first common step in the biosynthesis of valine, leucine, and isoleucine in plants and microorganisms. AHAS is the target of several classes of herbicides. In the present study, the role of three well-conserved arginine residues (R141, R372, and R376) in tobacco AHAS was determined by site-directed mutagenesis. The mutated enzymes, referred to as R141A, R141F, and R376F, were inactive and unable to bind to the cofactor, FAD. The inactive mutants had the same secondary structure as that of the wild type. The mutants R141K, R372F, and R376K exhibited much lower specific activities than the wild type, and moderate resistance to herbicides such as Londax, Cadre, and/or TP. The mutation R141K showed a strong reduction in activation efficiency by ThDP, while the mutations R372K and R376K showed a strong reduction in activation efficiency by FAD in comparison to the wild type enzyme. Taking into account the data presented here and the homology model constructed previously [Le *et al.* (2004) *Biochem. Biophys. Res. Commun.* 317, 930–938], it is suggested that the three amino acid residues studied (R141, R372, and R376) are located essentially at the enzyme active site, and, furthermore, that residues R372 and R376 are possibly responsible for the binding of the enzyme to FAD.

Key words: acetohydroxy acid synthase, conserved arginine, homology model, site-directed mutagenesis, tobacco.

Abbreviations: AHAS, acetohydroxy acid synthase; mAHAS, mutant AHAS; wAHAS, wild type AHAS; CD, circular dichroism; FAD, flavine adenine dinucleotide; GSH, glutathione; GST, glutathione S-transferase; IPTG, isopropyl- β -D-thiogalactoside; PCR, polymerase chain reaction; TP, triazolopyrimidine sulfonamide; ThDP, thiamine diphosphate.

Acetohydroxy acid synthase (AHAS, EC 2.2.1.6—formerly known as EC 4.1.3.18; also known as acetolactate synthase, ALS) catalyzes the condensation of two molecules of pyruvate to give rise to 2-acetolactate in the first step of the valine and leucine biosynthetic pathways, and the condensation of pyruvate and 2-ketobutyrate to yield 2-aceto-2-hydroxybutyrate in the second step of isoleucine biosynthesis (1). AHAS requires three cofactors for its catalytic activity, thiamine diphosphate (ThDP), flavin adenine dinucleotide (FAD), and divalent metal ion, Mg²⁺ or Mn²⁺. AHAS has been demonstrated to be the target of several classes of modern and potent herbicides, including sulfonylureas (2, 3), imidazolinones (4), and triazolopyrimidines (5, 6).

Previously, the AHAS gene from tobacco has been functionally expressed in *Escherichia coli*, and the enzyme has been purified (7). Various herbicide-resistant AHAS mutants from several plants and microorganisms have been obtained (1, 8). In our laboratory, studies on site-

directed mutagenesis have revealed several residues that are essential for the catalytic function as well as herbicide binding (9–15). Bartlett *et al.* has reported that 11% of the catalytic residues of structurally known enzymes are arginine (16). In addition, our study on the chemical modification of enzymes has shown that a single arginine residue is essential for catalytic activity in tobacco AHAS (17). Recently, the X-ray structure of the catalytic subunit of *Saccharomyces cerevisiae* AHAS has been reported (18, 19). Based on the yeast AHAS X-ray structure, we successfully obtained a reliable molecular model of tobacco AHAS (9) by using the Deep View and Swiss-Model servers (20).

In the present study, we have identified the conserved arginine residues of tobacco AHAS by multiple sequence alignment, carried out site-directed mutagenesis of three conserved residues that are likely to be located at the cofactor-binding site(s) (R141, R372, and R376) of tobacco AHAS, and analyzed the effects of mutations on the kinetic parameters, enzyme structure, and inhibition by herbicides. The data obtained are also discussed with respect to the homology model.

*Present address: The Microbial Engineering Laboratory, National Food Research Institute, Kannondai 2-1-12, Tsukuba, Ibaraki 305-0856.

†To whom correspondence should be addressed. Tel: +82-43-261-2308, Fax: +82-43-267-2306, E-mail: jdchoi@chungbuk.ac.kr

MATERIALS AND METHODS

Materials—Bacto-tryptone, yeast extract, and Bacto-agar were purchased from Difco Laboratories (Detroit, USA). Restriction enzymes were purchased from Takara Shuzo Co. (Shiga, Japan) and Boehringer-Mannheim (Mannheim, Germany). GSH, ThDP, FAD, α -naphthol, and creatine were obtained from Sigma Chemical Co. (St. Louis, USA). Thrombin protease and epoxy-activated Sepharose 6B were obtained from Pharmacia Biotech (Uppsala, Sweden). *E. coli* XL1-blue cells containing the expression vector pGEX-AHAS were kindly provided by Dr. Soo-Ik Chang (Chungbuk National University, Cheongju, Korea). Oligonucleotides were obtained from Genotech (Daejeon, Korea). Londax (a sulfonylurea herbicide) and Cadre (an imidazolinone herbicide) were kindly provided by Dr. Dae-Whang Kim (Korea Research Institute of Chemical Technology, Daejeon, Korea). TP, a triazolopyrimidine derivative, was obtained from Dr. Sung-Keon Namgoong (Seoul Women's University, Seoul, Korea).

Multiple Sequence Alignment of AHAS Sequences—The multiple sequence alignment was done using ClustalW (21) as described previously (14) using a database set consisting of 39 AHAS sequences (9).

Site-Directed Mutagenesis—Site-directed mutagenesis of tobacco AHAS was performed directly on the plasmid derived from pGEX-2T containing tobacco AHAS cDNA using the PCR megaprimer method (22). All DNA manipulations were carried out according to the techniques reported previously (23). The first PCR was carried out with oligonucleotide primer NKB2 and each mutagenic fragment as internal primers with the underlined bases changed: NKB2, 5'-CCC**GGATCCT**CAAAGTCAATA-3'; R141A, 5'-CGCAACGTGCTGCCAGCTCAC-3'; R141F, 5'-CTACC**ATTC** CACGAGCAGG-3'; R141K, 5'-CTACCA-**AAA** CACGAGCAGG-3'; R372F, 5'-CATTTGGGGTGTTC-TTTGATG-3'; R372K, 5'-CATTTGGGGTGA**AGTTT**GATG-3'; R376F, 5'-GAGGTTT**GATGATTT**CGTTACTGG-3'; R376K, 5'-GAGGTTT**GATGATAA**AGTTACTGG-3'. The bold bases in the NKB2 primer comprise a *Bam*HI restriction site. The resulting DNA was subjected to a second PCR with the universal primer NKB1 5'-CATC-TCC**GGATC**CATGTCCACTACCCAA-3'. The PCR products were double digested with *Nco*I and *Bgl*II, and cloned into the expression vector, which was prepared from *Nco*I/*Bgl*II-excised pGEX-wAHAS. The resulting pGEX-mAHAS was used to transform *E. coli* strain XL1-Blue cells according to standard CaCl_2 transformation instructions (23). Transformants were identified by digestion of the plasmid with *Bam*HI, followed by sequencing to ensure the correct base mutation.

DNA Sequence Analysis—DNA sequencing was carried out by the dideoxy chain-termination procedure (24) at Macrogen, Inc. (Seoul, Korea).

Expression and Purification of Tobacco wAHAS and mAHAS—Bacterial strains of *E. coli* BL21-DE3 cells containing the expression vector pGEX-AHAS were grown at 37°C in Luria-Bertani (LB) medium containing 50 $\mu\text{g}/\text{ml}$ ampicillin to an OD_{600} of 0.7–0.8. Expression of the pGEX-AHAS gene was induced by adding 0.1–0.3 mM isopropyl-D-thiogalactoside (IPTG). Cells were grown for an additional 4 h at 30°C, and harvested by centrifuga-

tion at $5,000 \times g$ for 30 min. Purification of wAHAS and mAHAS was carried out as described previously by Chang *et al.* (7). The isolated protein was identified by SDS-PAGE analysis (25), and the protein concentration was determined by the method of Bradford (26).

Enzyme Assay—Enzyme activities of the purified wAHAS and mAHAS were measured according to the method of Westerfeld (27) with some modification as reported previously (28). The reaction mixture contained 50 mM potassium phosphate buffer (pH 7.5), 1 mM ThDP, 10 mM MgCl_2 , 20 μM FAD, 100 mM pyruvate, and the enzyme in the absence or presence of various concentrations of cofactors or inhibitors. The values of V_{max} and K_m for the substrate were determined by fitting the data to Eq. 1, while the values of activation constant (K_c) were obtained by fitting the data to Eq. 2.

$$v = V_{\text{max}}/(1 + K_m/[S]) \quad (1)$$

$$v = V_0 + V_{\text{max}}/(1 + K_c/[C]) \quad (2)$$

In these equations, v is the reaction velocity, V_{max} is the maximum velocity, V_0 is the activity due to the trace of cofactors present in the apo-enzyme solution, K_m is the Michaelis-Menten constant, K_c is the activation constant, $[S]$ is the substrate concentration, and $[C]$ is the added cofactor concentration. K_i^{app} values were determined by fitting to the data to Eq. 3.

$$v_i = v_0/(1 + [I]/K_i^{\text{app}}) \quad (3)$$

In this equation, v_i and v_0 represent the rate in the presence or absence of inhibitor, respectively, and $[I]$ is the concentration of the inhibitor. K_i^{app} is the apparent K_i , which is the concentration of inhibitor resulting in 50% inhibition under standard assay conditions, and is also known as IC_{50} . All fittings and data analyses were carried out with the program Sigma Plot 8.0 (Systat Software Inc., California, USA).

Spectroscopic Studies—Absorption and fluorescence emission measurement were performed as previously reported (9, 14). CD spectra were recorded on a Jasco J-710 Spectropolarimeter set at 20–50 mdeg sensitivity, 1 nm resolution, 3 units accumulation, and 5 s response, at a scanning speed of 200 nm/min (see figure's legends for details).

Analysis of Structural Models—The structure of the homology model (9) was analyzed by Deep View (20). Structural illustrations were created from coordinate files with Deep View and Molw PDB Viewer 4.0 with Showcase (<http://www.molimg.com>).

RESULTS

Arg141 Mutants—To determine the functions of the R141 residue, three mutants were constructed, R141A, R141F, and R141K. While the three mutants expressed and purified to homogeneity showed a similar molecular weights to that of the wild type (data not shown), the R141A mutant was inactive under various assay conditions, while the R141F mutant retained only trace activity, and the R141K mutant retained 1% of activity. The most notable feature of the R141K mutant is that its acti-

Table 1. Kinetic parameters of the wild type and mutant enzymes used in the present study.

Enzymes	V_{\max} (U mg ⁻¹)	K_m (pyruvate, mM)	V_{\max}/K_m	Affinity for FAD		Affinity for TPP	
				V_0	$(V_{\max} - V_0)/K_{\text{FAD}}$	V_0	$(V_{\max} - V_0)/K_{\text{TPP}}$
wAHAS	1.55 ± 0.05	11.7 ± 1.9	132.47 × 10 ⁻³	0.96	28.5 × 10 ⁻³	0.86	23.6 × 10 ⁻³
R141A	No enzymatic activity						
R141F	0.006 ± 0.0005	116.8 ± 20.4	0.05 × 10 ⁻³	Not determined*			
R141K	0.014 ± 0.003	113.9 ± 33.1	0.12 × 10 ⁻³	0.006	0.38 × 10 ⁻³	0.004	0.21 × 10 ⁻³
R372F	0.015 ± 0.001	167.4 ± 38.6	0.09 × 10 ⁻³	0.004	1.5 × 10 ⁻³	0.00	0.24 × 10 ⁻³
R372K	0.33 ± 0.03	475.9 ± 106.6	0.69 × 10 ⁻³	0.002	1.6 × 10 ⁻³	0.00	2.4 × 10 ⁻³
R376F	No enzymatic activity						
R376K	0.041 ± 0.002	337.3 ± 45.9	0.12 × 10 ⁻³	0.00	2.1 × 10 ⁻³	0.00	0.74 × 10 ⁻³

*Not reliably determined due to too low activity.

Table 2. IC₅₀ values of the wild type and mutant enzymes.

Enzymes	Londax (nM)	Cadre (μM)	TP (μM)
wAHAS	13.0 ± 0.8	4.1 ± 0.5	29.3 ± 2.9
R141K	89.3 ± 15.8	14.8 ± 2.3	34.8 ± 3.2
R372F	49.4 ± 11.3	11.3 ± 3.9	108.8 ± 23.9
R372K	67.7 ± 5.7	8.62 ± 1.2	18.9 ± 0.7
R376K	76.8 ± 20.6	40.0 ± 14.4	52.5 ± 5.2

vation efficiency by ThDP (V_{\max}/K_{ThDP}) was substantially reduced (Table 1 and not shown). All mutations carried out at this residue produced only slight tolerance to the three tested herbicides (Table 2). In addition, the secondary structures of these mutants, as determined by CD spectroscopy, were similar to that of the wild type enzyme (data not shown). No bound FAD was detectable by either absorbance or fluorescence spectroscopy (Fig. 1 and data not shown). The homology model indicates that R141 is located likely near the ThDP-binding site of tobacco AHAS. The experimental data showed that mutations at this residue affect the binding of the enzyme to both cofactors, FAD and ThDP.

Arg372 Mutants—To determine the catalytic function of R372 residue, two mutants (R372F and R372K) were constructed. The two mutants were expressed and puri-

fied to homogeneity as judged by SDS-PAGE (data not shown). Both mutants were found to be active; however, the V_{\max} values of the R372F and R372K mutants for pyruvate were 1 and 21% that of the wild type, respectively (Table 1). Neither mutant was found to bind FAD by either absorbance or fluorescence spectroscopy (Fig. 1 and data not shown). The activation efficiencies by FAD (V_{\max}/K_{FAD}) of the two mutants were reduced substantially in comparison with the wild type. In addition, the activation efficiency by ThDP was also reduced profoundly. The R372F mutant was moderately resistant to Londax (a sulfonylurea) and TP (a triazolopyrimidine), while the R372K mutant was moderately resistant only to Londax (Table 2). The secondary structures of the two mutants were not significantly different from that of the wild type as determined from the far-UV CD spectra (data not shown). The near-UV CD spectra of the two mutants showed that while the overall conformation of the R372F mutant was similar to that of the wild type, the conformation of the R372K mutant was substantially different (Fig. 2). The experimental data showed that R372 may be imperative for FAD binding, and may also affect the binding of and activation by ThDP.

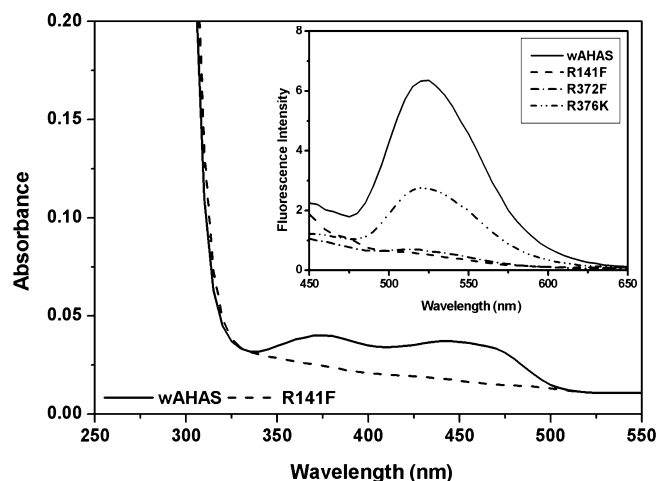


Fig. 1. Absorption and fluorescence spectra (inset) of wild type and mutant enzymes. The concentration of each enzyme for absorbance measurement was 0.8 mg protein/ml in 50 mM Tris-Cl buffer (pH 7.5), and for fluorescence measurement was 0.4 protein/ml in 50 mM Tris-Cl buffer (pH 7.5).

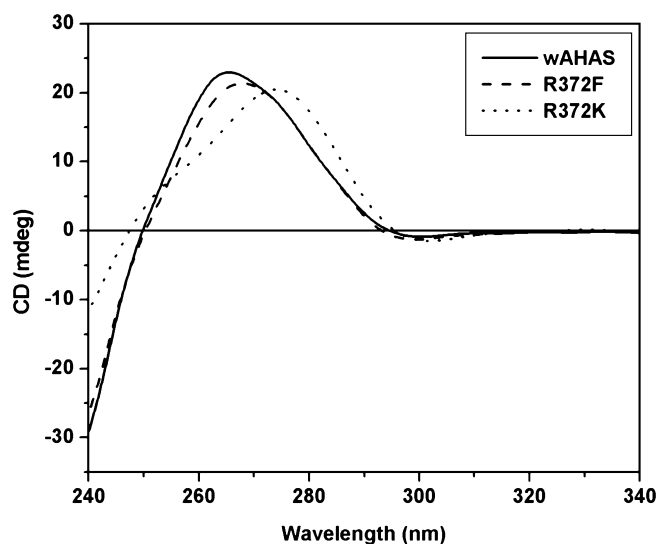


Fig. 2. Near UV CD spectra of wild type and R372 mutant enzymes. Each protein was present at a concentration of 0.20 mg/ml in 10 mM potassium phosphate buffer (pH 7.5). Samples were assayed in a 20-mm pathlength cylindrical quartz cell.

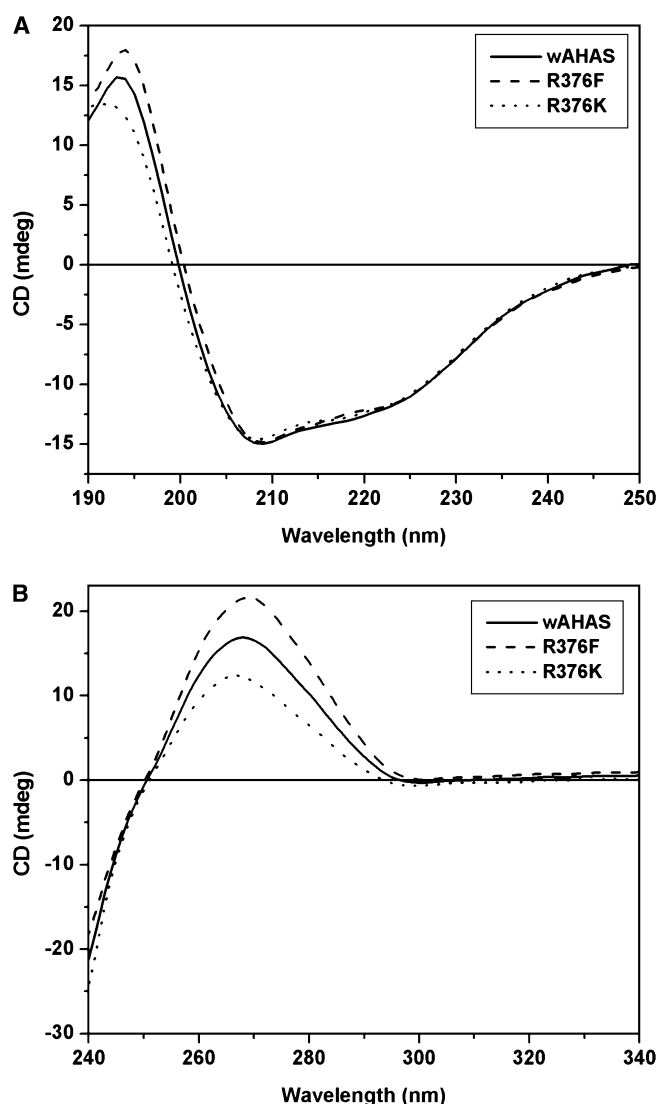


Fig. 3. Far-UV (A) and near-UV (B) CD spectra of wild type and R376 mutant enzymes. Each protein was present at a concentration of 0.20 mg/ml in 10 mM potassium phosphate buffer (pH 7.5). Samples were assayed in a 20-mm pathlength cylindrical quartz cell for near-UV region; the far-UV CD spectra were recorded using a 1-mm pathlength cylindrical quartz cell.

Arg376 Mutants—To understand the roles of residue R376 in mediating enzyme activity, two mutants R376F and R376K, were constructed. Both mutants were expressed as intact proteins; however, the R376F mutant was found to be inactive under various assay conditions. Although activity of the R376K mutant was detectable, it was extremely low in comparison with that of the wild type (Table 1). The absorbance and fluorescence spectra of the two mutants were measured. The presence of FAD in the R376K mutant was detectable in the fluorescence emission spectrum but was hardly observed in the absorbance spectrum (Fig. 1 and data not shown). The CD spectra of the two mutants (Fig. 3) show that the mutations did not cause any change in the secondary or tertiary structures of the enzyme. The mutant R376K showed moderate resistance to the three herbicides,

Londax (a sulfonylureas), Cadre (an imidazolinone), and TP (a triazolopyrimidine) (Table 2). Thus, the R376 residue seems to play an important role in the catalytic function and also affects herbicide binding.

DISCUSSION

Since the cofactors, ThDP and FAD, and substrates of AHAS are negatively charged, it is likely that the positively charged residues of the enzyme may be involved in cofactor and/or substrate binding. In addition, our chemical modification data showed that at least one arginine residue is essential for the catalytic activity of tobacco AHAS (17). Furthermore, Bartlett *et al.* reported that, among 178 structurally known enzymes, about 11% of the catalytic amino acid residues are arginine (16).

To determine the roles of arginine residues in AHAS that are essential for the catalytic functions of and herbicide binding to the enzyme, we identified conserved arginine residues by multiple sequence alignment using ClustalW. Three residues were selected for site-directed mutagenesis (R141, R372, and R376).

In the homology model constructed previously (9), residue R141 was found to be located near the ThDP cofactor (within 7 Å) and the ThDP-binding motif (Fig. 4). Residues R372 and R376 were found to be present in-close in proximity to the FAD molecule, and seemed to be involved in FAD binding (Fig. 5). To verify the predicted functions of the selected residues, site-directed mutagenesis was performed and 7 mutants were obtained of which 4 were active (Table 1).

Residue R141 is highly conserved among 39 AHAS sequences, and its sidechain is located close to the ThDP binding motif (see Fig. 4). Three mutants were constructed, of which the R141A and R141F mutants were found to be inactive, indicating that the residue is important for the catalytic activity. The other mutant (R141K) was active; however, its specific activity was extremely low in comparison with that of the wild type enzyme. None of the three mutants was detected with bound FAD by fluorescence spectroscopy (Fig. 1 and data not shown). The far-UV CD spectra also did not differ significantly from that of wild type AHAS, indicating no changes in secondary structure. The experimental data prove that the residue R141 is essentially located at the active site of the enzyme, and could probably affect the binding of both cofactors ThDP and FAD. Taken together with our previous work (9), it is likely that the loop of RHEQ is directly involved in the formation of the active site and may participate in the catalytic reaction.

Residues R372 and R376 form part of a highly conserved motif, ${}_{372}\text{RFDDR}_{376}$. The homology model showed that these two residues are located very close to the cofactor FAD, and are probably involved in the interaction with FAD. To study the functions of residue R372, two mutations were carried out with the resultant yield of R372F and R372K mutant forms. Although both mutants were active, the R372F mutant retained very low specific activity (1%) in comparison with the wild type enzyme (Table 1). The R372K mutant showed a reduction in activation efficiency by FAD. These data are in agreement with the homology model, since residue R372 was found to be involved in the binding of the diphosphate moiety of

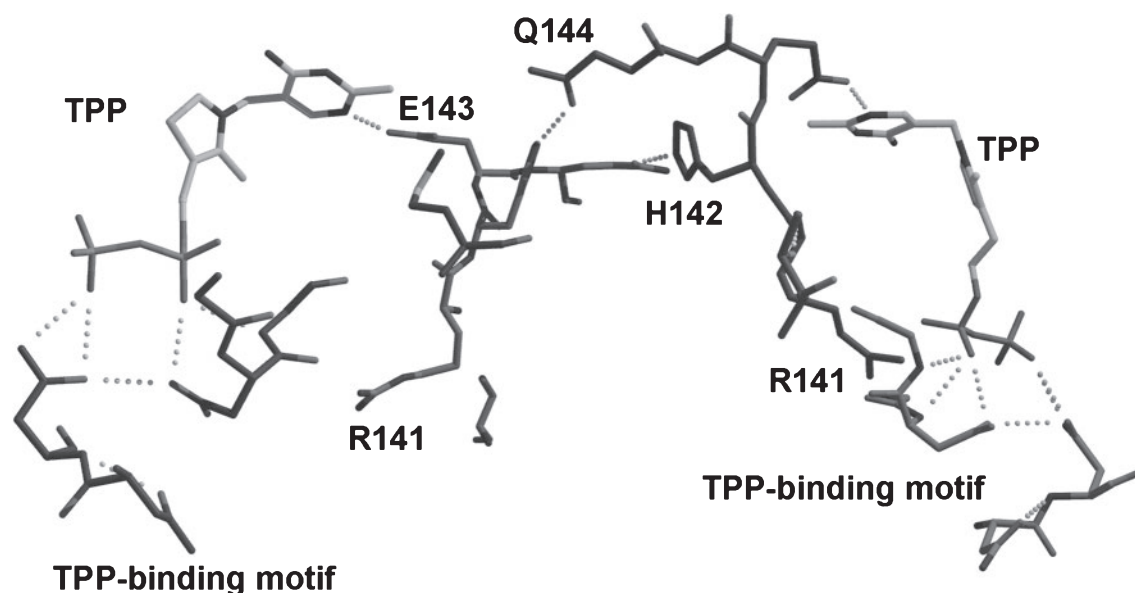


Fig. 4. **Structural model of the active site of tobacco AHAS.** Figure was created from the homology model using Molw 4.0.

the FAD molecule. The mutations at residue R372 also affected the binding affinity of and activation by cofactor ThDP as the activation efficiencies of the R372F and R372K mutants were 1 and 10% in comparison with that of the wild type, respectively. Since the homology model showed that residue R372 is quite far from the ThDP molecule, this effect may be indirect or may be the consequence of the reduced affinity for FAD.

Residue R376 is highly conserved among the 39 AHAS sequences. In addition, residue in yeast AHAS equivalent to tobacco R376 was identified to be involved in herbicide binding (1). Nevertheless, in our homology model, residue R376 seemed to be involved in binding with both FAD and the sulfonylurea herbicide. Recently, the residue Arg276 of *E. coli* AHAS II, which is equivalent to R376 in tobacco AHAS, was reported to be crucial to the specificity of the enzyme for condensation with a second ketoacid (29). This evidence prompted us to study the functions of residue R376 in tobacco AHAS. To explore

the roles of residue R376, two mutants, R376F and R376K, were constructed. The two mutants were expressed as intact proteins; however, only the R376K mutant was slightly active, while the R376F mutant remained inactive under various assay conditions. Since the R376F mutant did not retain any bound FAD (Fig. 1 and data not shown), and its CD spectrum resembled that of the wild type enzyme, residue R376 may be important for the catalytic function of the enzyme, and the positively charged group on the side chain may contribute to the activity.

Previously, AHAS was identified as a target for various classes of herbicides (2–6). Therefore, the inhibitions of the mutant AHASs by the three classes of herbicides, Londax (sulfonylurea), Cadre (an imidazolinone), and TP (a triazolopyrimidine) were determined. Since residue R141 is located at the active site and far away from the herbicide binding site (the model), it is not surprising that no strong resistance to herbicides was observed in

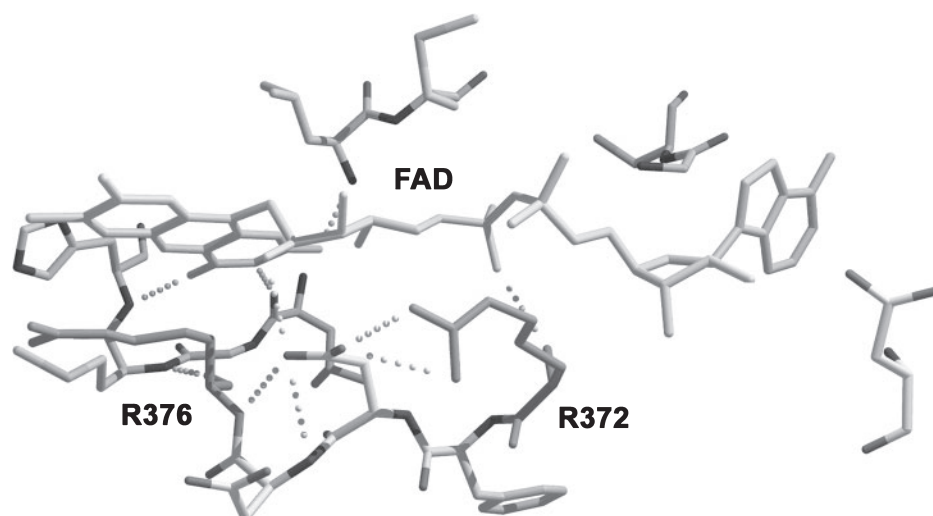


Fig. 5. **The FAD-binding site of the tobacco AHAS homology model.** Figure was created using Molw 4.0.

mutants of this residue. In contrast to other active mutants, the R376 mutant showed moderate resistance to the three classes of herbicides (Table 2). Thus, this residue probably also affects herbicide binding.

The homology model of tobacco AHAS shows that residues, R372 and R376 are located at the FAD-binding site, and, furthermore, that the R376 residue is also close to the herbicide-binding site (data not shown). Our experimental data show that residues R372 and R376 are important for catalytic activity, as they affect the binding with cofactor FAD. The conservative substitution mutant R376K showed moderate resistance to the three tested herbicides. Thus, the results are fairly consistent with the homology model. The herbicide binding site has also been reported to be proximal to the FAD binding site (1, 30). In the homology model constructed with bound sulfonylurea (chlorimuron ethyl, CIE), residue R376 was found to interact with the herbicide; on the other hand the mutation of R376 to phenylalanine inactivated the enzyme. Taking into account this evidence along with that reported by Engel *et al.* (29), it is likely that the herbicide sulfonylurea inhibits the enzyme by preventing residue R376 from being involved in condensation with the second ketoacid.

Taken together, the present results suggest that residue R141 is located at the active site and may affect the binding with cofactors ThDP and FAD, while residues R372 and R376 are located at the overlapping region of the FAD-binding site and are a common binding site for the three classes of herbicides.

We thank Dr. Dae-Whang Kim (Korea Research Institute of Chemical Technology, Korea) for providing us with Londax and Cadre, and Dr. Sung-Keon Namgoong (Seoul Women's University, Korea) for providing us with TP. This work was supported by Korea Research Foundation Grant KRF-2002-070-C0064.

REFERENCES

- Duggleby, R.G. and Pang, S.S. (2000) Acetohydroxyacid Synthase. *J. Biochem. Mol. Biol.* **33**, 1–36
- LaRossa, R.A. and Schloss, J.V. (1984) The sulfonylurea herbicide Sulfometuron is an extremely potent and selective inhibitor of acetolactate synthase in *Salmonella typhimurium*. *J. Biol. Chem.* **259**, 8753–8757
- Ray, J.B. (1984) Site of action of chlorosulfuron: Inhibition of valine and isoleucine biosynthesis of plants. *Plant Physiol.* **75**, 827–831
- Shaner, D.L., Anderson, P.C., and Stidham, M.A. (1984) Imidazolinones: potent inhibitors of acetohydroxy acid synthase. *Plant Physiol.* **76**, 545–546
- Gerwick, B.C., Subramanian, M.V., Loney-Gallant, V., and Chandler, D.P. (1990) Mechanism of action of the 1, 2, 4-triazolo[1, 5-a]pyrimidine. *Pestic. Sci.* **29**, 357–364
- Namgoong, S.K., Lee, H.J., Kim, Y.S., Shin, J.-H., Che, J.-K., Jang, D.Y., Kim, G.S., Yoo, J.W., Kang, M.-K., Kil, M.-W., Choi, J.-D., and Chang, S.-I. (1999) Synthesis of the quinoline-linked triazolopyrimidine analogues and their interactions with the recombinant tobacco acetolactate synthase. *Biochem. Biophys. Res. Commun.* **258**, 797–801
- Chang, S.-I., Kang, M.-K., Choi, J.-D., and Namgoong, S.K. (1997) Soluble overexpression in *Escherichia coli*, and purification and characterization of wild-type recombinant tobacco acetolactate synthase. *Biochem. Biophys. Res. Commun.* **234**, 549–553
- Chipman, D., Barak, Z., and Schloss, J.V. (1988) Biosynthesis of 2-aceto-2-hydroxy acids: acetolactate synthases and aceto-hydroxyacid synthases. *Biochim. Biophys. Acta* **1385**, 401–419
- Le, D.T., Yoon M.-Y., Kim, Y.T., and Choi, J.-D. (2004). Homology modeling and examination of the active site of tobacco acetolactate synthase. *Biochem. Biophys. Res. Commun.* **317**, 930–938
- Yoon, T.-Y., Chung S.-M., Chang S.-I., Yoon M.-Y., Hahn T.-R., and Choi J.-D. (2002) Roles of lysine 219 and 255 residues in tobacco acetolactate synthase. *Biochem. Biophys. Res. Commun.* **293**, 433–439
- Chong, C.-K., Shin, H.-J., Chang, S.-I., and Choi, J.-D. (1999) Role of tryptophanyl residues in tobacco acetolactate synthase. *Biochem. Biophys. Res. Commun.* **259**, 136–140
- Shin, H.-J., Chong, C.-K., Chang, S.-I., and Choi, J.-D. (2000) Structural and functional role of cysteinyl residues in tobacco acetolactate synthase. *Biochem. Biophys. Res. Commun.* **271**, 801–806
- Oh, K.-J., Park, E.-J., Yoon, M.-Y., Han, J.-R., and Choi, J.-D. (2001) Roles of histidine residues in tobacco acetolactate synthase. *Biochem. Biophys. Res. Commun.* **282**, 1237–1243
- Le, D.T., Yoon, M.-Y., Kim, Y.T., and Choi, J.-D. (2003) Roles of conserved methionine residues in tobacco acetolactate synthase. *Biochem. Biophys. Res. Commun.* **306**, 1075–1082
- Chong, C.-K. and Choi, J.-D. (2000) Amino acid residues conferring herbicide tolerance in tobacco acetolactate synthase. *Biochem. Biophys. Res. Commun.* **279**, 462–467
- Bartlett, G.J., Porter C.T., Borkakoti N., and Thornton J.M. (2002) Analysis of catalytic residues in enzyme active sites. *J. Mol. Biol.* **324**, 105–121
- Kim, S.-H., Park, E.-J., Yoon, S.-S., and Choi, J.-D. (2003) An active site arginine residue in tobacco acetolactate synthase. *Bull. Korean Chem. Soc.* **24**, 1799–1804
- Pang, S.S., Duggleby, R.G., and Guddat, L.W. (2002) Crystal structure of yeast acetohydroxyacid synthase: a target for herbicidal inhibitors. *J. Mol. Biol.* **317**, 249–262
- Pang, S.S., Guddat, L.W., and Duggleby, R.G. (2003) Molecular basis of Sulfonylureas herbicide inhibition of acetohydroxyacid synthase. *J. Biol. Chem.* **278**, 7639–7644
- Schwede, T., Kopp, J., Guex, N., and Peitsch, M.C. (2003) SWISS-MODEL: an automated protein homology-modeling server. *Nucleic Acids Res.* **31**, 3381–3385
- Thompson, J.D., Higgins, D.G., and Gibson, T.J. (1994) CLUSTALW: improving the sensitivity of progressive multiple sequence alignment through sequence weighting, positions-specific gap penalties and weight matrix choice. *Nucleic Acids Res.* **22**, 4673–4680
- Sarkar, G. and Sommer, S.S. (1990) “Megaprimer” method of site-directed mutagenesis. *Biotechniques* **2**, 404–407
- Sambrook, J., Fritsch, E.F., and Maniatis, T. (1989) *Molecular Cloning: A Laboratory Manual*, 2nd ed., Cold Spring Harbor Laboratory Press, Cold Spring Harbor, New York, USA
- Sanger, F., Nicklen, S., and Coulson, A.R. (1977) DNA sequencing with chain-terminating inhibitors. *Proc. Natl Acad. Sci. USA* **74**, 5463–5467
- Laemmli, U.K. (1970) Cleavage of structural proteins during the assembly of the head of bacteriophage T4. *Nature* **227**, 680–685
- Bradford, M.M. (1976) A rapid and sensitive method for the quantification of microgram quantities of protein utilizing the principle of protein-dye binding. *Anal. Biochem.* **72**, 248–254
- Westerfeld, W.W. (1945) A colorimetric determination of blood acetoin. *J. Biol. Chem.* **161**, 495–502
- Chong, C.-K., Chang, S.-I., and Choi, J.-D. (1997) Functional amino acid residues of recombinant tobacco acetolactate synthase. *J. Biochem. Mol. Biol.* **30**, 274–279
- Engel, S., Vyazmensky, M., Vinogradov, M., Berkovich, D., Bar-Ilan, A., Qimron, U., Rosiansky Y., Barak, Z., and Chipman, D.M. (2004) Role of a conserved Arginine in the mechanism of Acetohydroxy acid synthase: catalysis of condensation with a specific ketoacid substrate. *J. Biol. Chem.* **279**, 24803–24812
- Schloss, J.V., Ciskanik, L.M., and Van Dyk, D.E. (1988) Origin of the herbicide binding site of acetolactate synthase. *Nature* **331**, 360–362